Miscibility, Crystallization Kinetics, and Mechanical Properties of Poly(3-hydroxybutyrate-*co*-3-hydroxyvalerate)(PHBV)/Poly(3-hydroxybutyrate-*co*-4-hydroxybutyrate)(P3/4HB) Blends

Xiaojuan Wang, Zhifei Chen, Xianyu Chen, Jueyu Pan, Kaitian Xu

Multidisciplinary Research Center, Shantou University, Guangdong 515063, Shantou, China

Received 19 November 2008; accepted 25 July 2009
DOI 10.1002/app.31215
Published online 26 March 2010 in Wiley InterScience (www.interscience.wiley.com).

ABSTRACT: Poly(3-hydroxybutyrate-*co*-3-hydroxyvalerate)(PHBV)/poly(3-hydroxybutyrate-*co*-4-hydroxybutyrate) (P3/4HB) blend films were prepared by solvent-cast method. The nonisothermal crystallization results showed that PHBV and P3/4HB are miscible due to a single glass transition temperature (T_g), which is dependent on blend composition. The isothermal crystallization results demonstrate that the crystallization rate of PHBV becomes slower after adding amorphous P3/4HB with 19.2 mol% 4HB, which could be proved through depression of equilibrium melt point (T_m^o) from 183.7°C to 177.6°C. For pure PHBV and PHBV/P3/4HB (80/20) blend, the maximum crystallization rate appeared at 88°C and 84°C, respectively. FTIR analysis showed that PHBV/P3/4HB blend films would maintain the helical structure, similar to pure PHBV. Meanwhile, with increasing P3/4HB content, the inter- and intra-interactions of PHBV and P3/4HB decrease gradually. Besides, a lower elastic modulus and a higher elongation at break were obtained, which show that the addition of P3/4HB would make the brittle PHBV to ductile materials. J Appl Polym Sci 117: 838–848, 2010

Key words: PHBV; P3/4HB; miscibility; crystallization kinetics; morphology

INTRODUCTION

Biodegradable polyesters have received much attention because of the eco-friendly properties and potential use as industrial and biomedical materials in the last two decades.[1] Poly(3-hydroxybutyrate-*co*-3-hydroxyvalerate) (PHBV) is a biodegradable and biocompatible thermoplastic polymer, which can be produced by *Alcaligenes eutrophus* using pentanoic and butyric acids as the carbon sources.[2,3] The melting point of PHBV decreases from 178°C to 108°C with increasing 3-hydroxyvalerate (3HV) component from 0 to 95 mol%, and has a minimum value at 70°C when the 3HV content is 40 mol%.[4] The decrease of melt point means that the processing window becomes broad that would benefit the processing in industry. The crystallinity of PHBV is only slightly decreased when the 3HV content increase from 0 to 25 mol % because of the isodimorphism of PHBV.[5,6] However, PHBV is still too brittle to apply in industry when the HV content is low. Meanwhile, poly (3-hydroxybutyrate-*co*-4-hydroxybutyrate) (P3/4HB) was fermented successfully by *A. eutrophus* from the 4-hydrobutyric and butyric acid.[7,8] The physical property of P3/4HB is from semi-crystallization to amorphous elastomer depending on the 4-hydroxybutyrate (4HB) content.[4] The PHBV may be too rigid and brittle and lack of superior mechanical properties, which are required for biomedical and packaging film applications. In contrast, P3/4HB is elastomeric but has very low elastic modulus.[9] Several modifications have been proposed to improve their mechanical properties and processing of PHBV and P3/4HB, such as chemical modification and physical blending, in which blending is preferred because of the easy, fast, and low-cost working techniques.

Many researches have been done to study the miscibility and the crystallization property of PHBV to expand the potential applications in industry. On one hand, previous researchers revealed that PHBV was miscible with poly(vinylidene fluoride), poly (epichlorohydrin-*co*-ethylene oxide), and cellulose acetate butyrate.[10–12] On the other hand, PHBV was known as immiscible with other common type biodegradable polyesters such as poly(ε-caprolactone), poly(L-lactic acid), poly(butylene succinate), and poly(ethylene succinate).[13–17] However, the mechanical property

Correspondence to: K. Xu (ktxu@stu.edu.cn).
Contract grant sponsor: The Li Ka Shing Foundation, National Natural Science Foundation of China; contract grant number: 20474001.
Contract grant sponsor: National High Tech 863 Grant; contract grant number: 2006AA02Z242.

have not been significantly enhanced. Moreover, some functional monomers or polymers for example 4,4′-dihydroxydiphenyl propane, poly(p-vinyl phenol), and epoxidized natural rubber were used to blend with PHBV to study the crystallization property.[18–20] The hydrogen bonding was formed between the functional group and the carbonyl of PHBV in these blends systems. These functional materials acted as a physical cross-linked agent, herein reducing the crystallization rate of PHBV.

As far as we know, PHB[21] and PHBV (the content of HV is less than 37%)[4,22] belonged to $P2_12_12_1$-D_2^4 helix conformation in an orthorhombic system with $a = 5.76$ Å, $b = 13.20$ Å, and $c = 5.96$Å. Their unit cell contained the two helical chains in an antiparallel orientation rather than a single chain. The PHBV copolymer with the HV content from 0 to 37% crystallized in the P3HB lattice.

In this work, amorphous P3/4HB (19.2 mol% 4HB) was first chosen to blend with crystallized PHBV. Through differential scanning calorimetry (DSC), the nonisothermal crystallization was employed to investigate the miscibility and common crystallization property. Under different crystallization conditions, isothermal crystallization was used to further study the crystallization kinetics and the equilibrium melt point. We also used FTIR spectrum and the 2nd-derivative IR spectrum to investigate the molecular conformation of the PHBV/P3/4HB blend films.

EXPERIMENTAL

Materials

PHBV ($M_n = 252{,}000$, $M_w/M_n = 1.88$, estimated by GPC) with 5.7 mol% 3HV calculated by ^{1}H NMR was purchased from Tianan Biological Materials Co. (Zhejiang, China). P3/4HB ($M_n = 1{,}330{,}000$, $M_w/M_n = 1.30$, estimated by GPC) with 19.2 mol% 4HB was supplied by Tianjin Green Bioscience Materials Co. (Tianjin, China). The PHBV and P3/4HB samples were purified by dissolving in chloroform under 75°C for 3 h, followed by filtration and then precipitation in cold methanol. Chloroform in analytical grade was used without further purification. A series of PHBV/P3/4HB blend films with different mass ratios 100/0, 80/20, 60/40, 50/50, 40/60, 20/80, 0/100 was prepared through the conventional solvent-casting method. Typically, 1.5 g PHBV and 1.5 g P3/4HB were dissolved into 100 mL chloroform at 70°C for 3 h, and cast into the glass dish after cooling naturally to room temperature. The solvent was initially removed via evaporation at room temperature for 2 days, and the films were then vacuum dried at 80°C for 48 h to eliminate the residual chloroform completely. Finally, all samples were stored in glass desiccators at room temperature for more than 2 weeks before further analysis.

Characterization

Thermal analysis was performed on TA-Q100 DSC analyzer (Texas Intruments, USA) equipped with a mechanical cooler system under a nitrogen atmosphere and calibrated by indium. Two different procedures, including nonisothermal crystallization and isothermal crystallization, were employed to study the crystallization behavior of PHBV/P3/4HB blends.

For nonisothermal crystallization, the samples were heated from −50°C to 190°C at a heating rate of 10°C/min, held at 190°C for 3 min to destroy the thermal history. After quenched to −50°C at a cooling rate 80°C/min under dynamic nitrogen atmosphere, the tested sample was reheated to 190°C at a heating rate of 5°C/min. The glass transition temperature (T_g) and melt temperature (T_m) were obtained from the second heating trace. The sample was used to study the miscibility and conventional crystallization behavior of PHBV/P3/4HB blended film.

For isothermal crystallization, the samples were heated from −50°C to 190°C at a heating rate of 20°C/min, and then kept at 190°C for 3 min to destroy the thermal history. Followed by quenching to a certain crystallization temperature (T_c), the tested temperature was maintained at T_c until the crystallization completed. Finally, the sample was quenched to −50°C again, and reheated to 190°C at a heating rate of 20°C/min. The isothermal crystallization kinetics was studied and analyzed through the Avrami equation, whilst the equilibrium melt point was also calculated through the results of isothermal crystallization.

A polarizing optical microscope (POM; XPN-203Z, Shanghai Changfang Optical Instrument Co., Shanghai China) equipped with a hot stage was used to investigate the spherulitic morphology and crystal growth rate of PHBV/P3/4HB blends. Samples cut from the casting films were first heated to 190°C to destroy any thermal history, and then cooled rapidly to 90°C, and allowed to crystallize isothermally. The crystal growth rate G was calculated from the fitting slope of radius R with time t, i.e., $G = dR/dt$. The radius was measured with Photoshop CS3 software, and G was the average value of three spherulites at least. X-ray diffraction experiment was performed with a D8 Advance X-ray diffractometer (Bruker, Germany) using Cu Ka X-ray, with wave length $\lambda = 1.5406$ Å. A voltage of 40 kV and a current of 40 mA were used.

Transmission infrared spectra (FTIR) were measured by Nicolet IR 200 (Thermo Electron, USA)

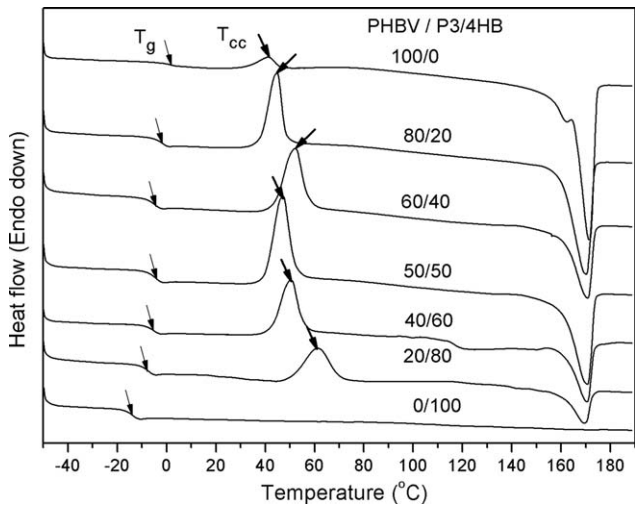

Figure 1 Melting behavior of PHBV/P3/4HB blends from the second heating run (5°C/min).

spectroscope: 3 mg blend film was dissolved in 1 mL chloroform, coated on a KBr pellet and dried before use. All samples were carried out with 64 scans at a resolution of 1 cm^{-1} at room temperature.

Mechanical property was determined by CMT-4000 universal testing machine (Shenzhen SANS, China) at room temperature, with the extension rate of 3 mm/min and maximal force 100N. The samples were prepared by a dumbbell-shape specimen cutter which was 6 mm in width, 40 mm in length and a thickness of 0.3–0.4 mm.

Morphology of the blend samples were studied through A JEOL JSM-6360 LA scanning electron microscope (JEOL, Japan). Surface images were recorded at a voltage of 10 kV; before observation, they were coated with a thin conductive layer of gold. Cross section samples for scanning electron micrographic observation were prepared by sample fracturing immediately after they were frozen by liquid nitrogen.

RESULTS AND DISCUSSION

Miscibility and nonisothermal crystallization of PHBV/P3/4HB blends

The miscibility plays an important role on the morphology, thermal properties, biodegradability, and mechanical properties for the PHBV/P3/4HB blends. A single glass transition temperature (T_g) depending on composition is the most wide and conventional criterion for the miscibility of a polymer blend. As introduced in the nonisothermal crystallization section, the DSC second heating trace of PHBV/P3/4HB blends and the thermal properties are shown in Figure 1 and Table I. One single endothermic melt peak at 171.6°C was corresponding to the melt point (T_m) of PHBV. No melting point for P3/4HB in second heating run indicated the P3/4HB was amorphous. Glass transition temperature (T_g) of pure PHBV and P3/4HB were displayed at 1.8°C and −13.7°C, respectively. The PHBV/P3/4HB blends exhibit a single T_g between the pure PHBV and pure P3/4HB. The tested T_g values are in good agreement with the calculated T_g by the Wood's equation:

$$T_g = w_{(\mathrm{PHBV})} T_{g(\mathrm{PHBV})} + \frac{k w_{(\mathrm{P3/4HB})} T g_{(\mathrm{P3/4HB})}}{w_{(\mathrm{PHBV})} + k w_{(\mathrm{P3/4HB})}} \quad (1)$$

where $w_{(\mathrm{PHBV})}$ and $w_{(\mathrm{P3/4HB})}$ are the weight fractions, $T_{g(\mathrm{PHBV})}$ and $T_{g(\mathrm{P3/4HB})}$ are the glass transition temperatures of PHBV and P3/4HB, respectively, T_g is the glass transition temperature of the blends, and k is an empirical adjustable parameter, in general $k = 0.64$.[23,24] The results (Fig. 2) show that the T_g of the blends increases with increasing PHBV contents in all blends. Namely, T_g is dependent on the composition of PHBV in the blends, which indicates that PHBV is miscible with P3/4HB in the blends. The crystallinity (X_c%) is defined as:

TABLE I
The Thermal Properties of PHBV and PHBV/P3/4HB Blends

PHBV/P3/4HB	T_g[a] (°C)	T_g[b] (°C)	T_{cc} (°C)	T_m (°C)	ΔH_m (J/g)	X_c[c] (%)	X_c[d] (%)	G[e] μm/s
100/0	1.8	1.8	41.1	171.6	83.8	57.1	73.2	2.24
80/20	−1.5	−0.5	44.9	170.2	65.8	44.9	64.5	1.32
60/40	−4.7	−3.0	52.1	170.8	44.8	30.6	56.8	1.08
50/50	−4.6	−4.5	47.2	170.7	46.4	31.7	45.6	0.93
40/60	−5.4	−6.0	50.4	170.4	31.2	21.3	40.5	0.65
20/80	−7.3	−9.5	61.3	169.5	16.7	11.4	35.4	0.36
0/100	−13.7	−13.7	–	–	–	–	20.3	–

[a] The glass transition temperature obtained from DSC determination.
[b] The glass transition temperature calculated from Wood's equation.
[c] Crystallinity calculated form DSC curve, $X_c = \frac{\Delta H_m}{\Delta H_m^0} \times 100\%$
[d] Crystallinity calculated form X-ray diffraction curve, $X_c = \frac{I_c}{I_c + I_a} \times 100\%$.
[e] Crystal growth rate (G) calculated from POM graph.

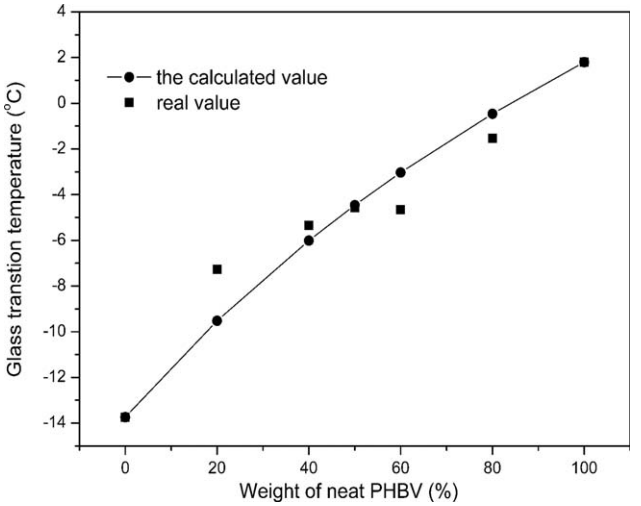

Figure 2 Glass transition temperature of the blends vs. PHBV content.

$$X_c = \frac{\Delta H_m}{\Delta H_m^\theta} \times 100\% \quad (2)$$

ΔH_m is the apparent fusion enthalpy of polymer obtained from the integral of the melting peaks in second heating run of DSC curve, and the ΔH_m^θ is the theoretical fusion enthalpy of a 100% crystalline PHBV which was taken as 146.6 J/g according to the previous work of Avella et al.[25] The cold crystallization temperature (T_{cc}) is generally increased with the increasing addition of P3/4HB, indicating the depression of PHBV crystallization. The ΔH_m and crystallinity is decreased gradually with the addition of P3/4HB. It implied that the amorphous P3/4HB may play a role of diluent to PHBV in the miscible melt and suppresses the crystallization of PHBV.[26]

Isothermal crystallization of PHBV and P3/4HB blends

Isothermal crystallization was employed mainly to investigate the crystallization properties and calculate crystallization activation and equilibrium melt point of PHBV/P3/4HB blends. The isothermal crystallization temperature of pure PHBV and PHBV/P3/4HB blend films was maintained at 90°C. The exothermal heat flow as a function of crystallization time t was recorded. The relative crystallinity X_t was calculated according to eq. (3):

$$X_t = \frac{(\int_0^t dH_c/dt)dt}{(\int_0^\infty dH_c/dt)dt} \quad (3)$$

where $\int_0^t dH_c/dt$ is the crystallization enthalpy from the initial time (t_0) to time t, $\int_0^\infty dH_c/dt$ is the crystallization enthalpy from the initial time (t_0) to fully crystallization (t_∞). These data can be obtained from the integral of the curve which is heat flow of isothermal crystallization versus crystallization time t. The relative crystallinity versus the crystallization time t for isothermal crystallization of pure PHBV and PHBV/P3/4HB blend films at 90°C is shown in Figure 3(a). By contrast to pure PHBV, the crystallization time of PHBV/P3/4HB blends becomes longer with increasing P3/4HB composition, especially when the content of P3/4HB is 50%.

Isothermal crystallization kinetics can be analyzed through the following Avrami equation:

$$1 - X_t = \exp(-kt^n) \quad (4)$$

$$\lg(-\ln(1 - X_t)) = \lg k + n1\text{gt} \quad (5)$$

where n is the Avrami exponent depending on the nature of nucleation and growth geometry for the crystal, and k is a crystallization rate constant involving the nucleation and growth rate parameters.[27,28] The plots of $\lg(-\ln(1 - X_t))$ versus lg t for PHBV/

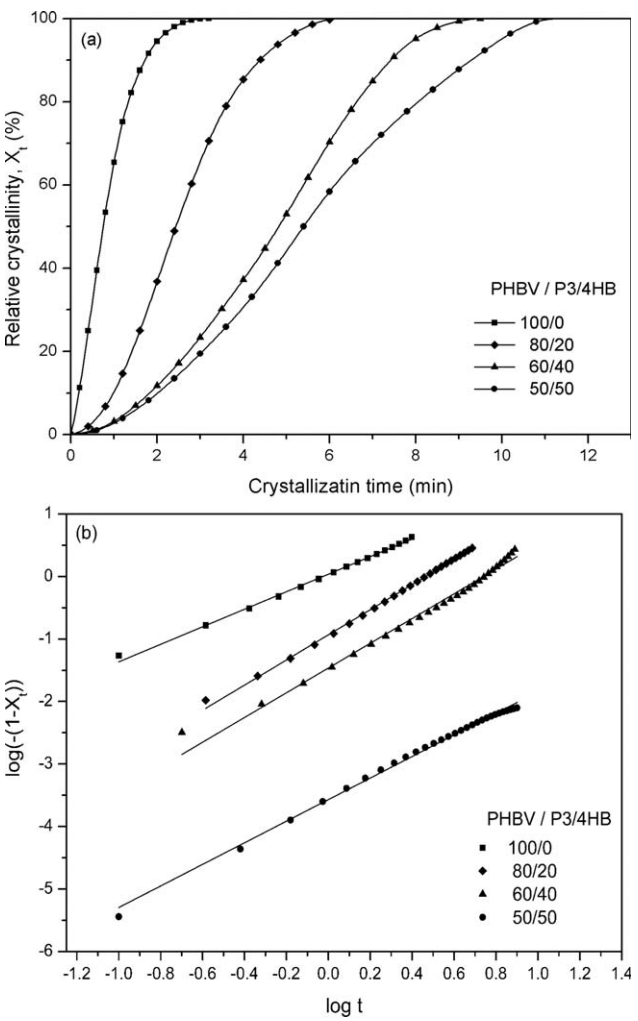

Figure 3 (a) Relative crystallinity X_t vs. crystallization time of the PHBV/P3/4HB blends at 90°C, (b) Avrami plots of the PHBV/P3/4HB blends at 90°C.

TABLE II
Kinetic Parameters of Isothermal Crystallization of PHBV and PHBV/P3/4HB Blends

PHBV/P3/4HB	T_c (°C)	n	k (min^{-n})	$t_{0.5}$ (min)	$1/t_{0.5}$ (min^{-1})
100/0	90	1.56	0.993	0.79	1.260
80/20	90	2.01	0.393	1.33	0.754
60/40	90	1.98	0.231	1.74	0.574
50/50	90	1.73	0.028	6.40	0.156
100/0	90	1.56	0.993	0.79	1.260
	88	1.49	1.074	0.74	1.343
	86	1.43	0.980	0.78	1.275
	84	1.44	0.757	0.94	1.063
	82	1.56	0.690	1.00	0.997
80/20	90	2.01	0.393	1.33	0.754
	88	1.91	0.452	1.34	0.747
	86	2.10	0.350	1.30	0.771
	84	1.81	0.556	1.39	0.718
	82	1.84	0.386	1.27	0.790

P3/4HB blends at 90°C were exactly in linear relationship which fit well with Avrami equation [Fig. 3(b)]. The Avrami parameters n and k can be obtained from the slope and the intercept of the double logarithmic curve, respectively (Fig. 3 and Table II). With increasing P3/4HB contents, the n value was elevated from 1.56 to 2.01. The results suggest that the primary crystallization processes should correspond from one-dimensional fibrillar growth geometry and homogeneous nucleation ($n = 1$) to two-dimensional circular diffusion-controlled growth ($n = 2$) in theory.[29] The real crystallization mode would be more complicated. The k value is reduced with increasing P3/4HB composition and the lowest k value was detected at P3/4HB content 50%. On one hand, the amorphous and miscible P3/4HB may dilute the crystalline PHBV and reduce the aggregation possibility of PHBV molecular chain. On the other hand, as described in FTIR section below, hydrogen-bond of PHBV became gradually weaker after the addition of amorphous P3/4HB, which means that the intermolecular interaction of PHBV and P3/4HB becomes weaker and results in reducing the crystallization rate of PHBV.

The crystallization half-time ($t_{0.5}$), which is determined by the time at $X_t = 50\%$, is calculated from the following kinetic parameters:

$$t_{0.5} = \left(\frac{\ln 2}{k}\right)^{1/n} \tag{6}$$

where n and k value are the parameters in the Avrami equation. The crystallization rate is described as the reciprocal of $t_{0.5}$, i.e., $1/t_{0.5}$, and the values of n, k, $t_{0.5}$, $1/t_{0.5}$ are listed in Table II. The value of $t_{0.5}$ increases with increasing the amorphous P3/4HB contents, whilst the trend of $1/t_{0.5}$ is consistent with trend of k. It revealed that the addition of amorphous P3/4HB weakens the interaction of intermolecular PHBV, reduces the crystallization rate of PHBV and increases the crystallization half-time.

The isothermal crystallization of pure PHBV at different crystallization temperature in the range of 82–90°C was also studied by DSC and analyzed through Avrami equation (Fig. 4 and Table II). There is no significant change of n value, which is around 1.5. The results had been analyzed above. The k value reached the maximum when isothermal crystallization temperature was 88°C, which can be explained through famous Lauritzen-Hoffmann theory.[30] The k is an overall crystallization rate constant depending on the nucleation and growth rate parameters. On one hand, the nucleation rate reduces with increasing T_c, which is a consequence of higher critical energy of nucleation at lower supercooling. On the other hand, the crystal growth rate involves the diffusion from molecular segment to the crystal surface. The increasing T_c would reduce the melt viscosity and thus increase chain mobility, result in the increase of the crystal growth rate. The two inverse effects can explain the presence of a maximum k at 88°C. Similarly, the isothermal crystallization of PHBV/P3/4HB (80/20) blend at the range of 82–90°C was also studied by DSC and analyzed through Avrami equation (Fig. 5 and Table II). The n value displays no apparent change around 2, but k value had a maximum value at 84°C, which also can be proved through the Lauritzen-Hoffmann theory.[30] Compared with pure PHBV, the depression of equilibrium melt points after the addition of P3/4HB (discussed in equilibrium melt points section in details) reduces the crystal growth rate, and the dilution effect of P3/4HB also reduces the nucleation rate. The overall crystallization rate k of PHBV/P3/4HB (80/20) blend film is lower than pure PHBV at the same T_c. For pure PHBV and PHBV/P3/4HB (80/20) blend, the values of $t_{0.5}$ and $1/t_{0.5}$ demonstrates some change with the

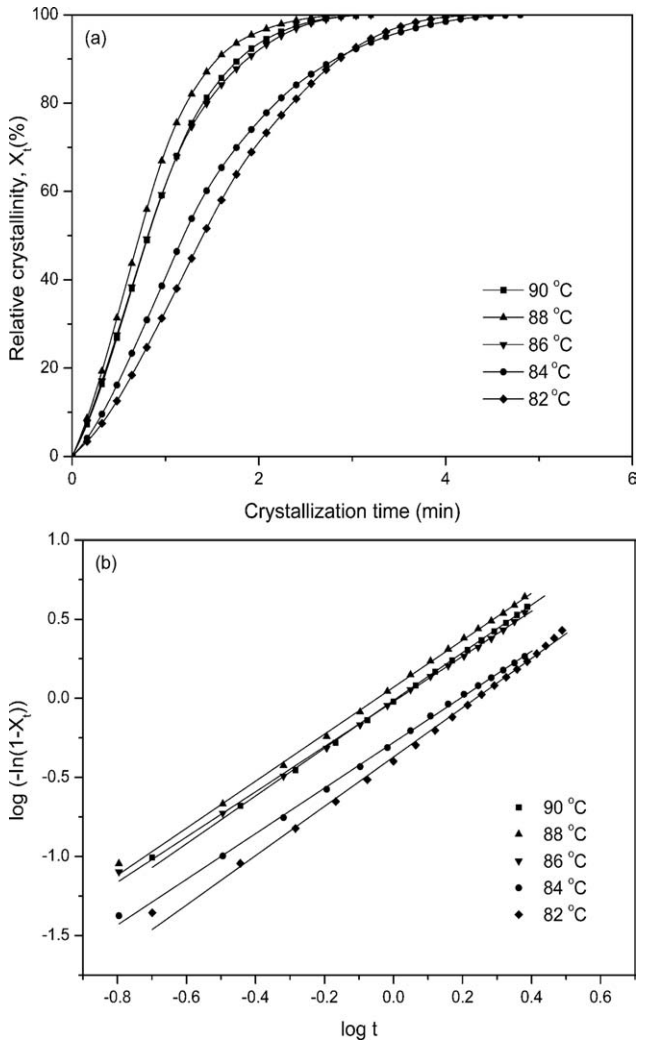

Figure 4 (a) Relative crystallinity X_t vs. crystallization time for pure PHBV at different crystallization temperature, (b) Avrami plots of pure PHBV at different crystallization temperature.

temperature, which indicated that the change of crystallization temperature does impose effect on $t_{0.5}$ and $1/t_{0.5}$ (Table II).

Morphology observation of pure PHBV and PHBV/P3/4HB blends

The spherulitic morphology and crystal growth rate of pure PHBV and PHBV/P3/4HB blends at 90°C were measured with polarizing optical microscopy (Fig. 6). Pure and blended PHBV spherulites exhibit concentric extinction band structures with clear Maltese cross birefringence pattern, and the band spacing changes with the P3/4HB content.[10] Generally, as reported in the literature, the banded structure of spherulite is due to the existence of twisted lamellae resulting from stress build up during crystallization and probably occurring within disordered fold surfaces of polymer crystals.[31,32] Similarly, it can be seen that the PHBV and P3/4HB were miscible and phase separation did not take place.

The spherulitic growth rate of pure and blended PHBV was also measured by the change of radius with time. Both pure and blended PHBV spherulite radius showed a linear growth with crystallization time until contacting with other spherulites during the crystallization process. The results (Table I) show that the spherulitic growth rates of pure and blended PHBV decrease with increasing the P3/4HB content. With increasing the content of P3/4HB, the reduction of the crystal nucleus density and spherulite growth rate results in the decrease of the crystallization rate which is consistent with the result of DSC analysis at the same temperature.

Equilibrium melt point analysis of pure PHBV and PHBV/P3/4HB blends

The equilibrium melt point (T_m^o) can be calculated by Hoffman-Weeks equation:

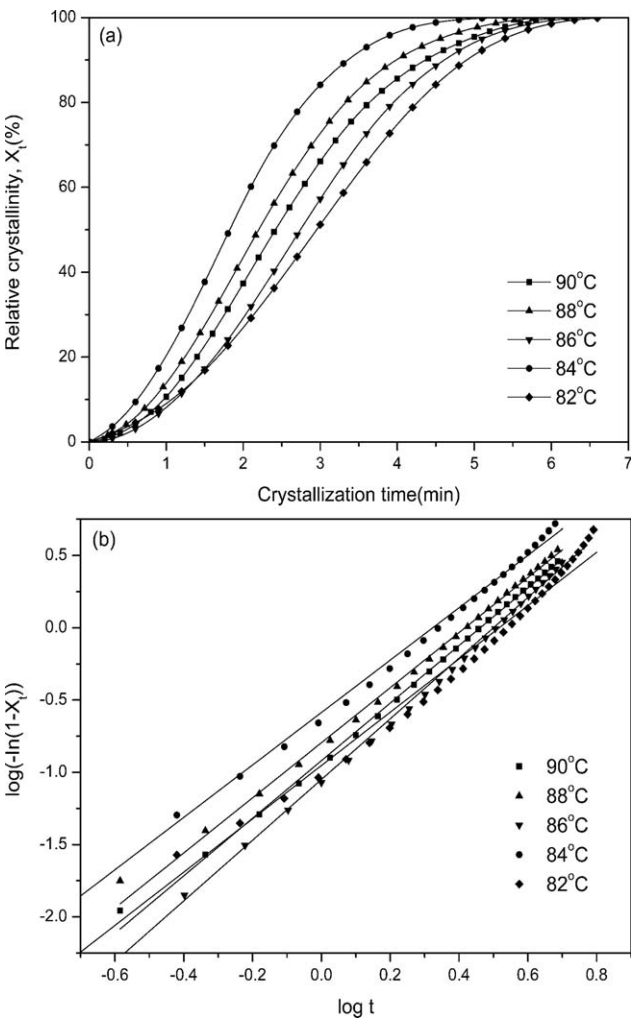

Figure 5 (a) Relative crystallinity X_t vs. crystallization time for PHBV/P3/4HB (80/20) blend at different crystallization temperature, (b) Avrami plots of PHBV/P3/4HB (80/20) blend at different crystallization temperature.

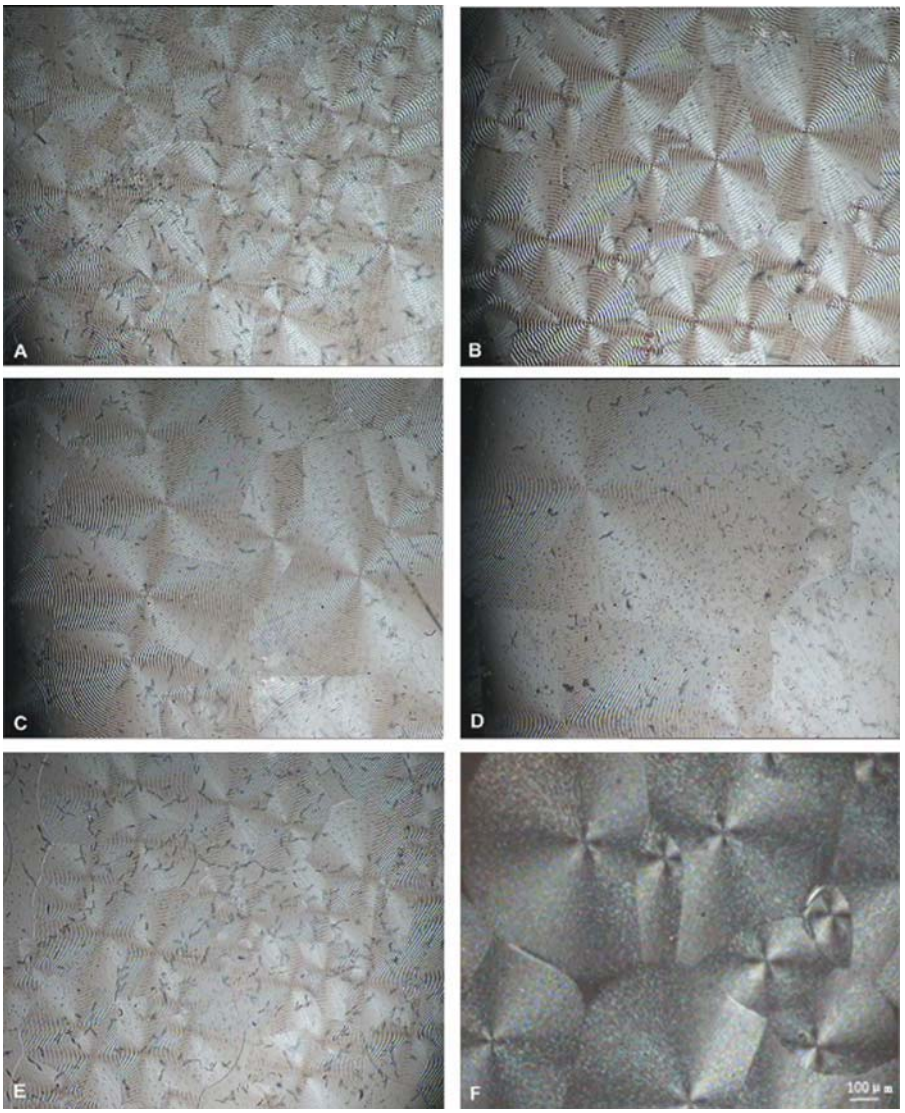

Figure 6 POM micrographs of pure PHBV and PHBV/P3/4HB blends at 90°C. A: 100/0, B: 80/20, C: 60/40, D: 50/50, E: 40/60, F: 20/80. [Color figure can be viewed in the online issue, which is available at www.interscience.wiley.com.]

$$T_m = \left(1 - \frac{1}{\beta}\right) T_m^o + \frac{1}{\beta} T_c \tag{7}$$

where β is the ratio of final to initial lamellar thickness and represents ability of the lamellar crystal to thicken, and the value of $1/\beta$ is between 0 ($T_m = T_m^o$ for all T_c, in the case of most stable crystal) to 1 ($T_m = T_c$ in the case of inherently unstable crystal).[11,33] The values of $1/\beta$ obtained from the slops were 0.318 and 0.302 for pure PHBV and PHBV/P3/4HB (80/20) blend, respectively. It was noted that addition of P3/4HB did not give remarkable change on crystal stability of PHBV. Besides, T_m^o was obtained from the intersection of the line T_m which was a function of T_c for pure PHBV and PHBV/P3/4HB blends, and the line $T_m = T_c$ (Fig. 7). Actually, there exist two melting peaks after isothermal crystallization (data not shown). The higher melting peak is ascribed to the melting process of the recrystallized crystallites, while the lower melting peak corresponds to the melting of original crystals existed prior to DSC scan.[34] The lower melting point was chosen to calculate the equilibrium melting points according to the previous analysis.[35] The values of T_m^o for pure PHBV and PHBV/P3/4HB (80/20) blend were 183.7°C and 177.6°C, respectively. It means that the value of T_m^o is depressed with increasing the content of P3/4HB. Generally, the supercooling degree, which describes as $T_m^o - T_c$, is considered as the thermodynamic driving force for the crystal growth process.[30] The lower value of $T_m^o - T_c$ obtains, the slower crystal growth rate encounters. This explains why the crystallization rate k becomes lower with increasing the content of P3/4HB (Fig. 3).

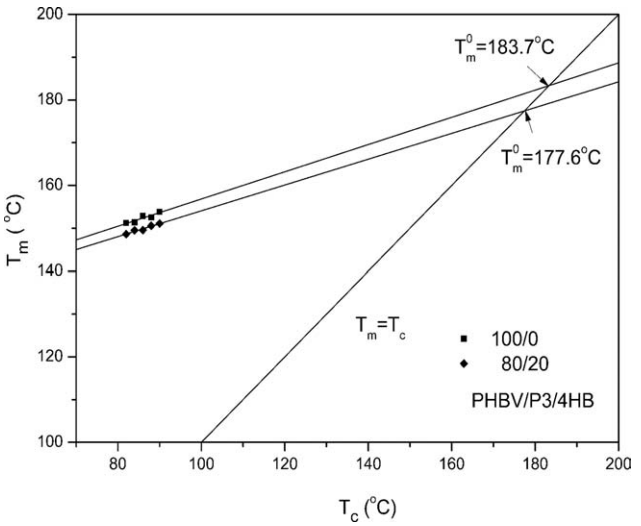

Figure 7 Hoffman-Weeks plots of pure PHBV and PHBV/P3/4HB (80/20) blend.

Structure of pure PHBV and PHBV/P3/4HB blends

The crystal structure of pure and blended PHBV was also investigated by X-ray diffraction (Fig. 8). According to Doi's research, PHBV (the content of HV is less than 37%) and P3/4HB (the content of 4HB is less than 49%) belongs to $P2_12_12_1$-D_2[4] helix conformation in an orthorhombic system. The crystallization structures of them are P(3HB) lattice.[4] The main diffraction peaks appeares around 13.6, 17.0, 22.4, 25.6, and 30.7°, which are corresponded to (020), (110), (111), (121), and (002) crystallographic planes, respectively.[18] It can be seen that both pure and blended PHBV exhibit peaks at almost the same locations, indicating that blending with P3/4HB does not modify the crystal structure of PHBV, and P3/4HB exists in an amorphous state and is excluded from the crystal region of PHBV.

The crystallinity of blend films were calculated by the ratio of the five crystallization peaks areas to all the peaks areas. The results were listed in Table I. The crystallinity calculated from DSC and X-ray diffraction gives the similar trend except for pure P3/4HB. However, the crystallinity obtained by X-ray diffraction is general higher than that obtained by DSC. The two different kinds of testing mechanisms result in the difference of the results. Usually, we use crystallinity data from DSC to define the crystallinity or amorphous of polymers. From DSC data, it revealed that pure P3/4HB is amorphous, because there is no melting peak in the DSC second heating run, even though there are some X-ray diffractions observed. peaks in the X-ray diffractions are as mentioned above.

FTIR spectra of pure PHBV and PHBV/P3/4HB blends

Generally, FTIR is sensitive to conformational and local molecular environment of polymers. It have been extensively used as a convenient and powerful tool for investigating the chemical structure. The broad C–H stretching vibration of crystalline PHBV presents at 2975 cm^{-1}, while that of P3/4HB is located in 2981 cm^{-1} [Fig. 9(a)]. The bands at 1722 cm^{-1} and 1738 cm^{-1} are assigned to C=O stretching vibration crystalline part of PHBV and amorphous part of P3/4HB, respectively. Moreover, C–O–C stretching vibration bands of P3/4HB is placed at 1304 cm^{-1} and 1260 cm^{-1}, while the bands at 1228 cm^{-1} and 1278 cm^{-1} with two small shoulder peaks at 1290 cm^{-1}, 1263 cm^{-1} should be assigned to that of PHBV [Fig. 9(b)]. The second derivative of C–H stretching vibration was used to expatiate further the structure of PHBV/P3/4HB blends [Fig. 9(c)]. The spectra and their second derivatives of the PHBV blends films were similar to previous report of Murakami et al.[36] Their second derivatives of PHBV blend films in the 3015–2960 cm^{-1} regions are assigned to CH_3 asymmetric, whereas the 2945–2925 cm^{-1}, 2855–2865 cm^{-1} regions are attributed to CH_2 antiasymmetric and CH_3 symmetric stretching vibration, respectively. The five bands at 3010, 2997, 2981, 2975, 2967 cm^{-1} should be attributed to the CH_3 asymmetric stretching vibration. The band at 2981 cm^{-1} increased with the composition of P3/4HB should be assigned to CH_3 asymmetric stretching vibration of the P3/4HB amorphous moiety. The other four bands should be attributed to that of PHBV crystalline portion.[37] In general, CH_3 asymmetric stretching bands shows in the 2975–2950 cm^{-1} regions. Thus, the CH_3 asymmetric stretching bands for PHBV blends displays a slightly blue shift to 3010 cm^{-1}. According to the former research on the structure,[4,22] PHBV (HV content less than 37%) was assumed to form the helical molecular conformation and crystallize in the P3HB lattice. Two left handed helical molecules were packed together with

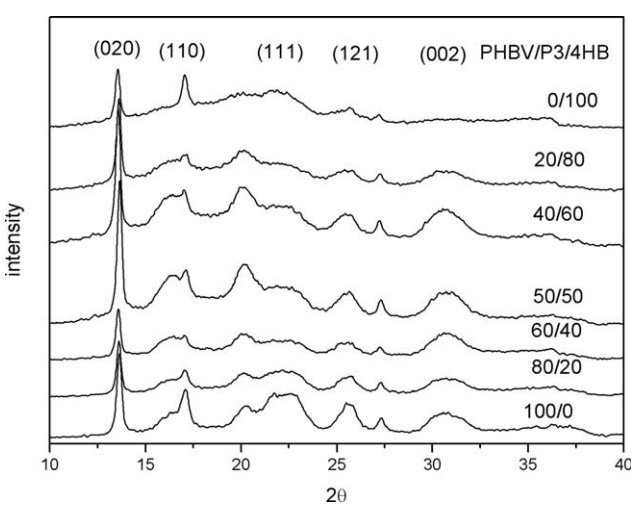

Figure 8 X-ray diffraction patterns of pure PHBV and PHBV/P3/4HB blends.

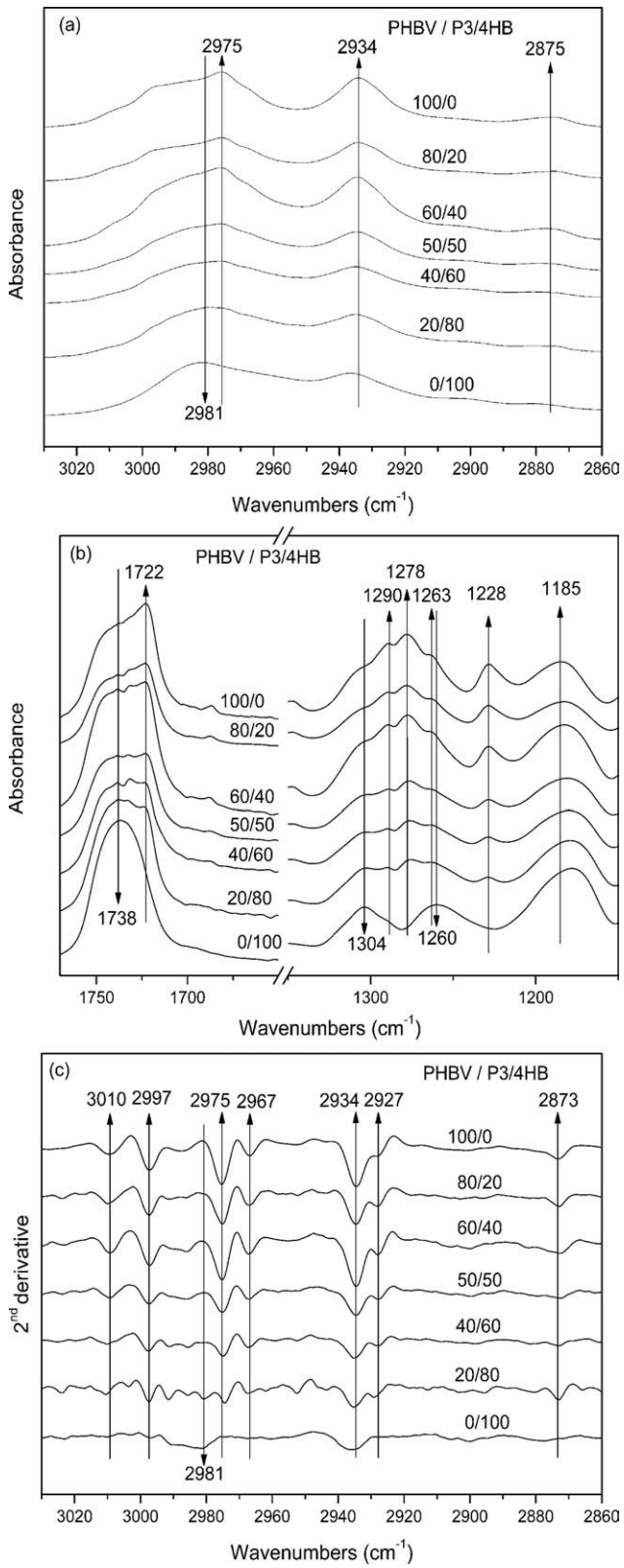

Figure 9 FTIR spectra of PHBV/P3/4HB blends (a) C—H stretching band regions; (b) C=O and C—O—C stretching band regions; (c) the second derivatives of the spectra (a).

the ester group in the anti-parallel orientation.[21] The blue shift would be attributed to intermolecular or intramolecular C–H···O=C hydrogen bond between the CH_3 group of one helix and C=O group of the another helix existed in the PHBV/P3/4HB blend films.[37,38] When P3/4HB content is increased, CH_3 asymmetric stretching peaks in 3010 cm^{-1} become gradually smaller. For pure P3/4HB, the CH_3 asymmetric stretching peaks locate at 2981 cm^{-1}. No apparent shift observed indicates that hydrogen bond does not exist. It showed that the hydrogen bond becomes gradually weaker when increasing the amorphous P3/4HB contents, because the addition of amorphous P3/4HB leads to the separation of two helixes in the anti-parallel orientation. These results would hint that the blends could maintain the helix structure, but the structure may be deformed to some extent. Furthermore, the C–H···O=C hydrogen bond become gradually weaker, and reduces the interaction of PHBV with P3/4HB when increasing the P3/4HB contents.

Mechanical properties of pure PHBV and PHBV/P3/4HB blends

Mechanical test experiments were performed to investigate the effect of blending with P3/4HB on the mechanical properties of PHBV (Table III). Elastic modulus decreases from 1406.7 MPa to 72.9 MPa and the elongation at break increases from 2.3% to 1381.8%, while the trend of tensile strength is irregular with the contents of P3/4HB increased from 0% to 100%. With increasing mass ratio of amorphous P3/4HB, the T_g of the amorphous region and the crystallization rate of PHBV decreases gradually. This results in the decrease in the elastic modulus and the increase of elongation at break markedly. Taking PHBV/P3/4HB (40/60) blend film for example, it showed a 3-times decrease in elastic modulus, and a 290-times increase in elongation at break compared with pure PHBV. The tailor-made PHBV/P3/4HB blend films could improve the elastic modulus compared with pure P3/4HB and increase the

TABLE III
Mechanical Properties of PHBV and PHBV/P3/4hb Blends

PHBV/P3/4HB blend films	Tensile strength (δ_t) (MPa)	Elastic modulus (E) (MPa)	Elongation at break (ε_b) (%)
100/0	18.8	1406.7	2.3
80/20	20.9	1142.2	52.5
60/40	16.8	1031.3	259.9
50/50	17.6	766.5	356.1
40/60	24.8	460.4	673.7
20/80	21.4	177.5	956.9
0/100	22.9	72.9	1381.8

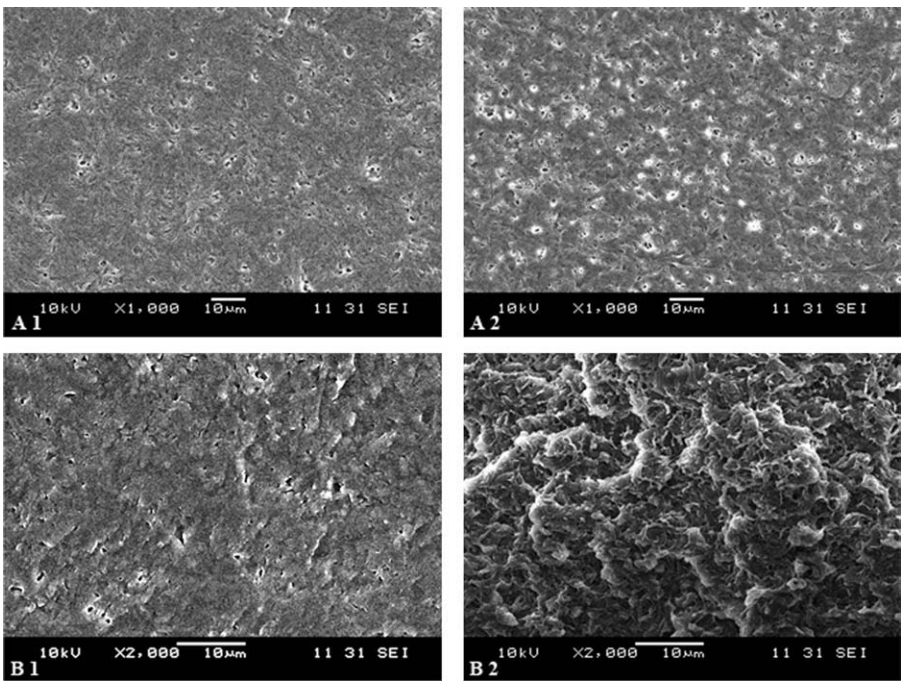

Figure 10 SEM micrographs, A1, A2: the surface of pure PHBV and PHBV/P3/4HB (80/20) blend, respectively; B1, B2: the cross section of pure PHBV and PHBV/P3/4HB (80/20) blend, respectively.

elongation at break than pure PHBV. In other words, the addition of amorphous P3/4HB overcomes the rigidity of pure PHBV and the resulted PHBV-based blend films become ductile.

SEM morphology of pure PHBV and PHBV/P3/4HB blends

SEM was used to study the morphology and fracture behavior of PHBV/P3/4HB blends. SEM observations on the surfaces of pure PHBV and PHBV/P3/4HB (80/20) blend films are shown in Figure 10. The surface of pure PHBV film is smooth and seems to be ordered flower-like pattern. Compared with pure PHBV, the surface of PHBV/P3/4HB (80/20) blend film presents disordered pattern. There was no obvious phase-separation of the blend. This phenomenon is another significant proof that the amorphous P3/4HB is miscible with pure PHBV. Figure 10 also gives SEM micrographs of the fracture surfaces of pure PHBV and PHBV/P3/4HB (80/20) blend films after frozen in liquid nitrogen. In terms of fracture patterns, pure PHBV seems to be a smooth surface, and PHBV/P3/4HB (80/20) blend film tends to be a rough surface. The smooth fracture surface indicates the brittle fracture behavior of pure PHBV, whereas the rough surface implies the ductile fracture behavior of PHBV/P3/4HB (80/20) blend film.[39] The analysis above demonstrates that PHBV fracture behavior changes from brittle fracture to ductile fracture after addition of P3/4HB. These phenomena are well consistent with the mechanical results, further verifies the potential applications of PHBV/P3/4HB blend films as a ductile materials.

CONCLUSIONS

Nonisothermal crystallization study through DSC revealed that PHBV is miscible with amorphous P3/4HB. At a given crystallization temperature 90°C, the Avrami exponent n changes from 1.56 to 2.01, and the crystallization rate k of PHBV decreases distinctively after adding amorphous P3/4HB, which can also be proved through the decrease of intermolecular interaction and the depression of equilibrium melt point. The FTIR analysis showed that the addition of amorphous P3/4HB still maintains the helical structure of PHBV. At experimental range from 82°C to 90°C, the maximal crystallization rate appeared at 88°C and 84°C for pure PHBV and PHBV/P3/4HB (80/20), respectively. Besides, PHBV/P3/4HB (40/60) blend film showed a 3-fold decrease in elastic modulus and a 290-fold increase in elongation at break compared with pure PHBV. The fracture behavior changes from brittle to ductile fracture. The blended films overcome the rigidity of pure PHBV and the low elastic modulus of P3/4HB which would satisfy the applications in industry.

References

1. Xu, K. T.; Zhao, S. J. Chin J Appl Environ Biol 1995, 1, 86.
2. Doi, Y.; Tamaki, A.; Kunioka, M.; Soea, K. J Chem Soc Chem Commun 1987, 16, 631.

3. Doi, Y.; Tamaki, A.; Kunioka, M.; Soea, K. Appl Microbiol Biotechnol 1988, 28, 330.
4. Kunioka, M.; Tamaki, A.; Doi, Y. Macromolecules 1989, 22, 694.
5. Mitomo, H.; Barham, P. J.; Keller, A. Polym Commun 1988, 29, 112.
6. Bloembergen, S.; Holden, D. A.; Hamer, G. K.; Bluhm, T. L.; Marchessault, R. H. Macromolecules 1986, 19, 2865.
7. Doi, Y.; Kunioka, M.; Nakamura, Y.; Soea, K. Macromolecules 1988, 21, 2722.
8. Doi, Y.; Segawa, A.; Kunioka, M. Int J Biol Macromol 1990, 12, 106.
9. Avella, M.; Martuscelli, E.; Raimo, M. J Mater Sci 2000, 35, 523.
10. Qiu, Z. B.; Fujinamib, S.; Komurab, M.; Nakajimab, K.; Ikeharaa, T.; Nishi, T. Polymer 2004, 45, 4355.
11. Zhang, L. L.; Goh, S. H.; Lee, S. Y.; Hee, G. R. Polymer 2000, 41, 1429.
12. Buchanan, C.; Gedon, S.; White, A.; Wood, M. Macromolecules 1992, 25, 7373.
13. Qiu, Z. B.; Yang, W.T.; Ikehara, T.; Nishi, T. Polymer 2005, 46, 11814.
14. Jenkins, M. J.; Cao, Y.; Howell, L.; Leek, G. A. Polymer 2007, 48, 6304.
15. Ferreira, B. M.; Zavaglia, C. A.; Duek, E. A. J Appl Polym Sci 2002, 86, 2898.
16. Qiu, Z. B.; Ikehara, T.; Nishi, T. Polymer 2003, 44, 7519.
17. Miao, L. Q.; Qiu, Z. B.; Yang, W.T.; Ikehara, T. React Funct Polym 2008, 68, 446.
18. Chen, C.; Wu, H.; Peng, S.; Wang, X. Y.; Dong, L. S.; Xin, J. H. Polymer 2004, 45, 6275.
19. Zhang, L.; Goh, S. H.; Lee, S. T. J Appl Polym Sci 1999, 74, 383.
20. Hana, C. C.; Ismaila, J.; Kammer, H. W. Polym Degrad Stab 2004, 85, 947.
21. Yokouchi, M.; Chatani, Y.; Tadokoro, H.; Teranishi, K.; Tani, H. Polymer 1973, 14, 267.
22. Sato, H.; Nakamura, M.; Padermshoke, A.; Yamaguchi, H.; Terauchi, H.; Ekgasit, S.; Noda, I.; Ozaki, Y. Macromolecules 2004, 37, 3763.
23. Wood, L. A. J Polym Sci 1958, 28, 319.
24. Zheng, Z.; Bei, F. F.; Tian, H. L.; Chen, G. Q. Biomaterials 2005, 26, 3537.
25. Avella, M.; Larota, G.; Martuscelli, E.; Raimo, M. J Mater Sci 2000, 35, 829.
26. Luo, R. C.; Xu, K. T.; Chen, G. Q. J Appl Polym Sci 2007, 105, 3402.
27. Avarmi, M. J Chem Phys 1939, 7, 1103.
28. Avarmi, M. J Chem Phys 1940, 8, 2124.
29. Chen, Q. Y.; Yu, Y. N.; Na, T. H.; Zhang, H. F.; Mo, Z. S. J Appl Polym Sci 2002, 83, 2528.
30. John, I.; Lauritzen, Jr; Hoffman, J. D. J Appl Phys 1973, 44, 4340.
31. Keith, H. D.; Padden, F. J. Jr, J Appl Phys 1964, 35, 1270.
32. Keith, H. D.; Padden, F. J. Polymer 1984, 25, 28.
33. Hoffman, J. D.; Weeks, J. J. J Res Natl Bur Stand 1962, 66, 13.
34. Qiu, Z. B.; Ikehara, T.; Nishi, T. Polymer 2003, 44, 3095.
35. Liu, W. J.; Yang, H. L.; Wang, Z.; Dong, L. S.; Liu, J. J. J Appl Polym Sci 2002, 86, 2145.
36. Murakami, R.; Sato, H.; Dybal, J.; Iwat, T.; Ozaki, Y. Polymer 2007, 48, 2672.
37. Sato, H.; Dybal, J.; Murakami, R.; Noda, I.; Ozaki, Y. J Mol Struct 2005, 35, 744.
38. Matsuura, H.; Yoshida, H.; Hieda, M.; Yamanaka, S.; Harada, T.; Shin-Ya, K. J Am Chem Soc 2003, 12, 13910.
39. Lu, J. M.; Qiu, Z. B.; Yang, W.T. Polymer 2007, 48, 4196.